21. Lofberg, A., Frennet, A., Leclercq, G., Leclercq, L. & Giraudon, J. M. Mechanism of WO$_3$ reduction and carburization in CH$_4$/H$_2$ mixtures leading to bulk tungsten carbide powder catalysts. *J. Catal.* **189**, 189–183 (2000).

22. Park, S.-C., Park, H. & Lee, S. B. Reaction intermediate in thermal decomposition of 1,3-disilabutane to silicon carbide on Si(111). Comparative study of Cs$^+$ reactive ion scattering and secondary ion mass spectrometry. *Surf. Sci.* **450**, 117–125 (2000).

23. Zhang, Y. *et al.* Heterostructures of single-walled carbon nanotubes and carbide nanorods. *Science* **285**, 1719–1722 (1999).

24. Mayr, A., Yu, M. P. Y. & Yam, V. W.-W. Electronic communication between metal centers across unsaturated alkylidyne ligands. *J. Am. Chem. Soc.* **121**, 1760–1761 (1999).

25. Wang, D., Lunsford, J. H. & Rosynek, M. P. Characterization of a Mo/ZSM-5 catalyst for the conversion of methane to benzene. *J. Catal.* **169**, 347–358 (1997).

26. Tanaka, K.-I. & Takeshiro, N. Atomic-scale mechanism for the activation of catalyst surfaces. *J. Mol. Catal. A* **141**, 39–55 (1999).

27. Weck, M., Jackiw, J. W., Rossi, R. R., Weiss, P. S. & Grubbs, R. H. Ring-opening metathesis polymerization from surfaces. *J. Am. Chem. Soc.* **121**, 4088–4089 (1999).

28. Watson, K. J., Zhu, J., Nguyen, S. T. & Mirkin, C. A. Hybrid nanoparticles with block copolymer shell structures. *J. Am. Chem. Soc.* **121**, 462–463 (1999).

....

Recent mass balance of polar ice sheets inferred from patterns of global sea-level change

**Jerry X. Mitrovica*, Mark E. Tamisiea*, James L. Davis†
& Glenn A. Milne‡**

* *Department of Physics, University of Toronto, 60 St George Street, Toronto, M5S 1A7, Canada*
† *Harvard-Smithsonian Center for Astrophysics, 60 Garden Street MS42, Cambridge, Massachusetts 02138, USA*
‡ *Department of Geological Sciences, University of Durham, Science Laboratories, South Road, Durham DH1 3LE, UK*

....

Global sea level is an indicator of climate change[1–3], as it is sensitive to both thermal expansion of the oceans and a reduction of land-based glaciers. Global sea-level rise has been estimated by correcting observations from tide gauges for glacial isostatic adjustment—the continuing sea-level response due to melting of Late Pleistocene ice—and by computing the global mean of these residual trends[4–9]. In such analyses, spatial patterns of sea-level rise are assumed to be signals that will average out over geographically distributed tide-gauge data. But a long history of modelling studies[10–12] has demonstrated that non-uniform— that is, non-eustatic—sea-level redistributions can be produced by variations in the volume of the polar ice sheets. Here we present numerical predictions of gravitationally consistent patterns of sea-level change following variations in either the Antarctic or Greenland ice sheets or the melting of a suite of small mountain glaciers. These predictions are characterized by geometrically distinct patterns that reconcile spatial variations in previously published sea-level records. Under the—albeit coarse—assumption of a globally uniform thermal expansion of the oceans, our approach suggests melting of the Greenland ice complex over the last century equivalent to ~0.6 mm yr^{-1} of sea-level rise.

Gravitationally self-consistent sea-level changes arising from the growth or ablation of ice masses have been of interest for more than a century[10–12]. Woodward[10] demonstrated that the melting of an ice mass on a rigid Earth would lead to a highly non-uniform sea-level redistribution as a consequence of self-gravitation in the surface load. Indeed, sea level on a rigid Earth will drop within ~20° of a localized (point mass) ice melting event[12]. The sea-level theory was extended to include elastic deformations of the solid Earth (ref. 11 and others), culminating in the 'sea-level equation' derived and solved by Farrell and Clark[12].

We have computed sea-level redistributions associated with present-day mass variations in the Antarctic and Greenland ice complexes as well as melting from a suite of smaller land-based ice sheets and glaciers tabulated by Meier[13]. Our calculations are based on a new sea-level theory[14] that extends earlier work[12] to include a varying shoreline geometry and the influence of load-induced perturbations in the Earth's rotation vector. As we are concerned with sea-level variations associated with relatively rapid ice flux scenarios, we adopt a form of the theory suitable for an elastic Earth. The elastic and density structure of the model are adopted from PREM[15].

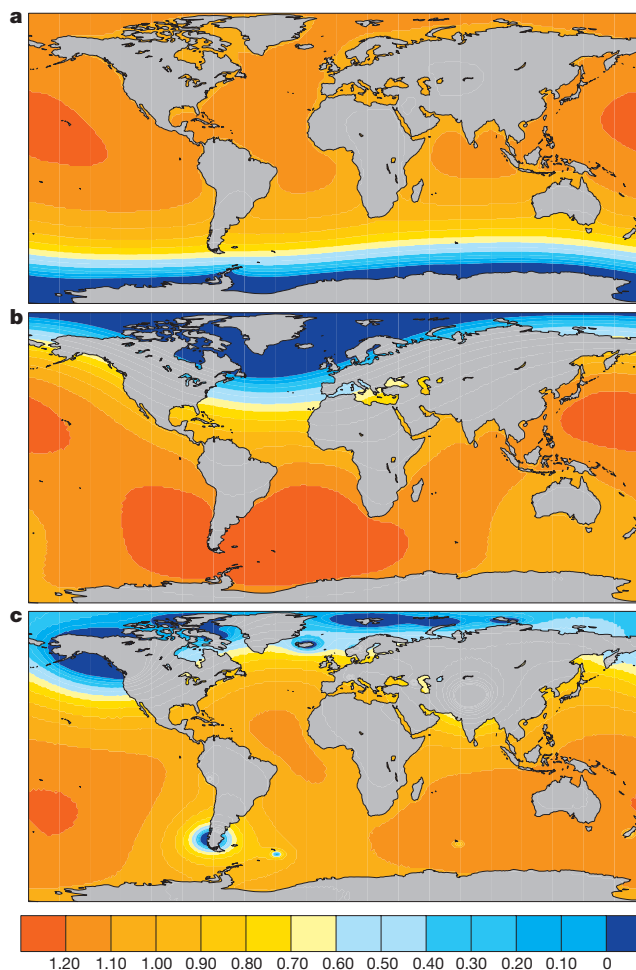Meier's sources[13] combine to provide a 'eustatic' sea-level rise of

Figure 1 Predicted geometries of sea-level change due to continuing ice mass variations. Normalized global sea-level variations were computed for the case of present-day ice mass variations in **a**, Antarctica, **b**, Greenland and **c**, melting of the mounting glaciers and ice sheets tabulated by Meier[13]. In **a** and **b** we assume that the mass variation is uniform over the two polar regions. The results are normalized by the equivalent eustatic sea-level change for each mass flux event (see text). Departures from a contour value of 1.0 reflect departures from the assumption that the sea-level distribution accompanying these mass flux events is uniform. Predictions are based on a new sea-level theory[14] solved using a pseudo-spectral algorithm[14,29] with truncation at spherical harmonic degree and order 512. This truncation corresponds to a spatial resolution of 40 km.

$0.46 \, \text{mm yr}^{-1}$. (In this context, the term eustatic is defined as the change in ocean volume, that is, the change in ice mass divided by the density of water, divided by the area of the ocean.) The integrated mass fluxes from the Antarctic and Greenland ice sheets are quantities of intense interest and they remain uncertain, even in sign[1,16]. Accordingly, we simply assume a uniform ice mass variation over the entire ice sheet in each case.

Figure 1 shows global maps of sea-level change due to mass variations in the Antarctic, Greenland and Meier's sources[13]. The frames in Fig. 1 are normalized by the eustatic sea-level variation associated with each of the three ice systems, which we denote by V_A, V_G, and V_M, respectively. We can thus write:

$$S_I(\theta, \phi) = V_A \times S_A^n(\theta, \phi) + V_G \times S_G^n(\theta, \phi) + V_M \times S_M^n(\theta, \phi) \quad (1)$$

where $S^n(\theta, \phi)$ are the maps of normalized sea-level change in Fig. 1, and $S_I(\theta, \phi)$ is the total predicted sea-level change from these three ice sources. The symbols θ and ϕ denote co-latitude and east-longitude, respectively. We have confirmed, using a series of more complex ice balance models for the Antarctic and Greenland[16–19], that the large-scale geometry of the computed sea-level redistribution is relatively insensitive to our assumption of a uniform ice mass variation over these regions.

Figure 1 confirms that present-day variations in polar ice mass will be accompanied by dramatic departures of sea level from eustasy. For the sake of discussion, let us assume that a melting event in Greenland contributes $1 \, \text{mm yr}^{-1}$ of eustatic sea-level rise. In this case, sea level will fall in the vicinity of Greenland, and it will rise by less than $0.2 \, \text{mm yr}^{-1}$ in Newfoundland, Britain and Fennoscandia (Fig. 1b). There is a strong north–south gradient throughout the Atlantic, northern Pacific and Mediterranean, with a maximum sea-level rise of $\sim 1.3 \, \text{mm yr}^{-1}$ obtained in the northern Pacific and southern Atlantic. (The asymmetry in the latitudinal position of the sea-level maxima in Fig. 1b is due to rotational perturbations associated with Greenland mass flux.) The dominant

cause of the non-uniform redistribution is self-gravitation in the surface mass load. Water will pile up in the near field of an ice mass as a consequence of gravitational attraction; as the ice melts the ocean will relax and water will tend to flow from the near field to the far field. The same physical effect is evident in the remaining two frames of Fig. 1: the ice mass variation near the South Pole will be accompanied by a significant north–south gradient in the Antarctic Ocean, whereas the sea-level response to the melting of mountain glaciers is characterized by regionally localized minima. In all cases, an expectation of eustasy is only met in spatially limited geographic bands. Thus, secular sea-level trends inferred from tide gauge records may, depending on their location, sample a sea-level redistribution due to polar ice melting that significantly departs from the 'eustatic' measure of the ice balance.

We have computed sea-level trends at $\sim 1,000$ sites in the database supplied by the Permanent Service for Mean Sea Level (PSMSL)[20] for each of the three mass flux scenarios in Fig. 1 (see Supplementary Information). PSMSL sites mainly reside in the Northern Hemisphere. In the case of Antarctic mass flux, sea-level change at most of the PSMSL sites ranges up to 20% larger than the eustatic value; the exceptions are the southern portions of Africa, Australia and South America, where the sites will sample a sea-level change markedly smaller than the eustatic value. The site-specific departures from eustasy are even more dramatic for Greenland ice mass variations; in this case, less than 30% of the sites will record a sea-level change that is within 10% of the eustatic value. Sea-level change induced by the variations of Greenland ice, as measured at sites in Spitsbergen, Iceland and Fennoscandia, hovers close to zero but increases toward the eustatic value southward from the UK to North Africa and from the Canadian east coast to Florida. There is a further dramatic departure from the eustatic value at sites in regions such as Alaska, Yukon and British Columbia. These sites are also close to some of the largest melting events in Meier's database[13] and thus exhibit extreme departures from the eustatic value that is associated with these sources of meltwater.

Estimates of global sea-level rise based on the analysis of tide gauge records require stringent site selection in order to avoid, for example, bias associated with interdecadal fluctuations and the contaminating effects of tectonic deformations[5]. In Fig. 2 we show predictions of sea-level change at 23 sites included in a recent tide gauge analysis[8]. In the case of Antarctic melting, these sites sample a sea-level change that ranges from 80% to 120% of the eustatic value. The departure from the eustatic value is large for European sites (numbers 1–8) in the case of Greenland melting. Indeed, the mean value for these sites is just 40% of the eustatic value.

The question arises as to whether geographic trends in observed tide gauge rates may be used to constrain meltwater contributions from the main ice reservoirs. A recent independent study[21] based on standard sea-level theory[12] has analysed $\sim 1,000$ sites in the Revised Local Reference PSMSL data set[20] for this purpose. We proceed by analysing the more carefully selected subset of sites treated in Fig. 2. Figure 3a shows secular sea-level rates at the 23 sites sampled in Fig. 2. The mean rate obtained from these sites is $1.5 \pm 0.1 \, \text{mm yr}^{-1}$, the weighted (by $1/\sigma^2$) root-mean-square value of the residuals (w.r.m.s.) about the mean is $0.4 \, \text{mm yr}^{-1}$, and the χ^2 residual value per-degree-of-freedom (henceforth χ^2) about the mean is 2.7. In Fig. 3b we show the same rates corrected for glacial isostatic adjustment (GIA) using the combination of ice and Earth model adopted in a number of earlier studies[4–6,8]. This model is characterized by the ICE-3G deglaciation history[22] and an Earth model with lower mantle viscosity of $2 \times 10^{21} \, \text{Pa s}$. The mean sea-level rate in this case is $1.8 \pm 0.1 \, \text{mm yr}^{-1}$, in agreement with ref. 8, and the w.r.m.s. and χ^2 about this mean are $0.4 \, \text{mm yr}^{-1}$ and 3.4, respectively. Thus, the GIA correction previously applied to these tide gauge rates does not improve the geographic consistency of the residuals. Finally, in Fig. 3c we show the rates in Fig. 3a corrected using a GIA model proposed[23] on the basis of fits to tide gauge
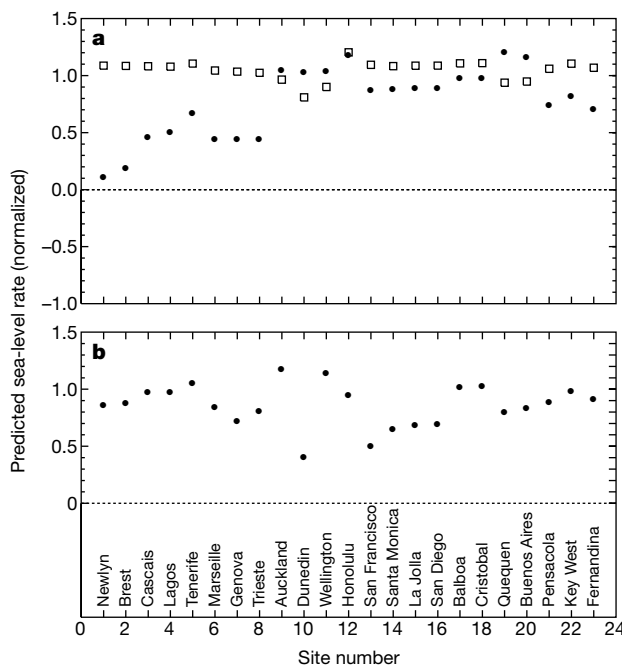

Figure 2 Predicted sea-level trends due to continuing ice mass variations at a subset of tide gauge sites. Shown are normalized sea-level rates from Fig. 1 for a selection of 23 sites (see labels at bottom) adopted in a recent tide gauge analysis[8]. (A final site, Lyttelton, New Zealand, is not included because it is characterized by an observed rate that is not consistent with rates at nearby sites). **a**, The square boxes and solid dots refer to predicted normalized sea-level rates for the case of Antarctic and Greenland ice mass variations. **b**, As in **a**, except for Meier's sources[13].

records along the US east coast. This GIA model is identical to that used in Fig. 3b, with the exception that the lower mantle viscosity is increased to 5×10^{21} Pa s. In this case, the mean rate is 1.5 ± 0.1 mm yr^{-1}, and the w.r.m.s. and χ^2 about this mean are reduced to 0.3 mm yr^{-1} and 2.1, respectively.

Next, we explore whether the geographic scatter evident in the GIA-corrected rates in Figs 3b and c can be reconciled on the basis of non-uniform sea-level change associated with polar melting events (Fig. 1). Following equation (1), we can denote the total sea-level change, at a site (θ_j, ϕ_j), attributable to all sources by:

$$S_T(\theta_j, \phi_j) = V_O \times S_O^n(\theta_j, \phi_j) + S_I(\theta_j, \phi_j) \qquad (2)$$

The first term on the right-hand side of equation (2) includes all contributions to sea-level change other (hence the subscript O) than the ice mass variations treated in Figs 1 and 2. Given the criteria used to select the 23 sites in Figs 2 and 3, we expect that these contributions will be dominated by ocean thermal expansion. Ideally, we can use equations (1) and (2) as the basis for a least-squares estimate of V_A, V_G and V_O, where the sea-level rates $S_T(\theta_j, \phi_j)$ are given by the 23 GIA-corrected tide-gauge rates in either Fig. 3b or c and the various normalized sea-level geometries $S^n(\theta_j, \phi_j)$ are known. The functions S_A^n, S_G^n and S_M^n are given in Fig. 1; however, the global geometry of ocean thermal expansion remains largely unknown.

As a preliminary application of the approach we proceed with a least-squares estimate of V_A, V_G and V_O by assuming that ocean thermal expansion contributes a eustatic sea-level rise (that is,

$S_O^n = 1$ over the oceans). Because the sea-level variation due to Antarctic mass flux is relatively flat for the 23 tide gauge sites we are considering (Fig. 2a), estimates for V_A and V_O will be highly correlated. Nevertheless, we have found that the least-squares procedure does yield a robust estimate of the sum $V_A + V_O$. The results of this calculation are shown by the solid lines superimposed on Fig. 3b and c. In Fig. 3b our best fit is obtained with $V_A + V_O = 0.99 \pm 0.13$ mm yr^{-1} and $V_G = 0.54 \pm 0.15$ mm yr^{-1}. Thus the total eustatic value (including V_M) is ~2.0 mm yr^{-1}. The analogous expressions for Fig. 3c are $V_A + V_O = 0.61 \pm 0.13$ mm yr^{-1} and $V_G = 0.60 \pm 0.15$ mm yr^{-1} for a total eustatic value of ~1.7 mm yr^{-1}.

In Fig. 3c, the χ^2 of the observations about the solid line (1.1) is significantly better (at greater than 90% confidence) than the χ^2 relative to the simple mean of these rates (2.1). Even a qualitative inspection of Fig. 3c indicates that many of the residual trends evident in the GIA-corrected sea-level rates are remarkably well fitted by our best-fit (solid line) prediction for $S_T(\theta, \phi)$. Furthermore, the mean predicted rate for the European sites (numbers 1–8) is ~0.5 mm yr^{-1} less than the mean predicted rate for the remaining sites. This difference is consistent with the observed trends on the same figure and provides a natural explanation for the long-standing observation that European sea-level rates are anomalously low[8,24–26].

The Meier[13] tabulation of smaller glaciers is probably incomplete and subject to error. Furthermore, the mass balance of these glaciers may not be purely secular. We have repeated the least-squares
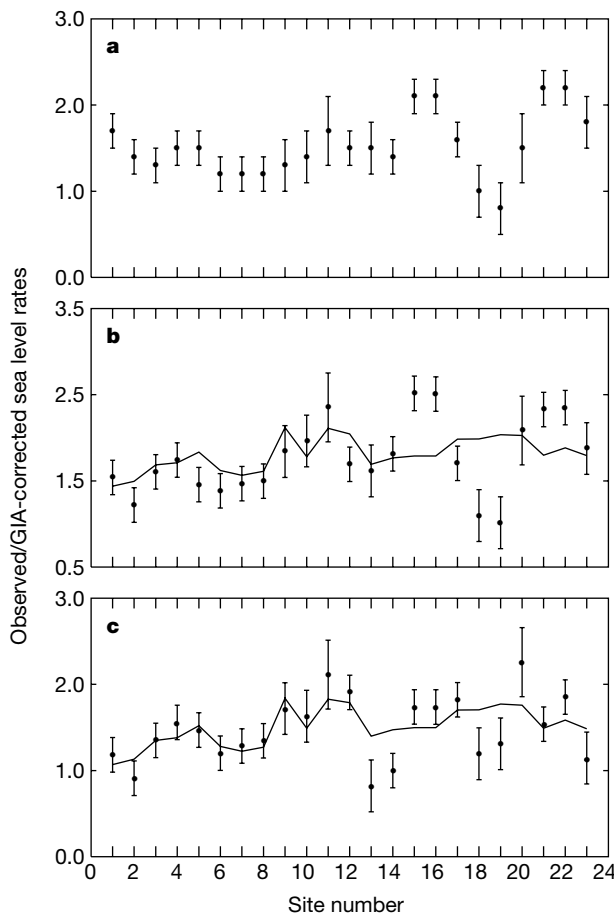

Figure 3 A new analysis of tide gauge records. **a**, Secular sea-level trends obtained (http://www.pol.ac.uk/psmsl/) from the PSMSL[20] tide gauge database for the set of 23 sites shown in Fig. 2. The error bars represent one-σ uncertainties. **b**, As in **a**, except for rates corrected using a GIA prediction based on an ice and Earth model combination adopted by previous studies[4–6,8] (see text). **c**, As in **b**, except that we adopt a GIA correction advocated[23] on the basis of its fit to geographic trends evident in tide gauge

records from the US east coast. The solid line in frames **b** and **c** represents the best-fitting prediction through the GIA-corrected residual tide gauge rates determined by a least-squares fit of these residuals to equation (2). The parameters in this fit are the equivalent eustatic sea-level variation associated with present-day ice mass variations in the Antarctic (V_A) and Greenland (V_G) as well as 'other' sources (V_0) described in the text. In this exercise V_M is set to a value of 0.46 mm yr^{-1}, as prescribed in the Meier database[13].

analysis in Fig. 3c by adopting a recent tabulation of 13 meltwater sources[27] in place of Meier's values for these sources (total V value of $0.34 \, \text{mm yr}^{-1}$) and have found that our estimates are not significantly altered ($V_A + V_O = 0.74 \pm 0.13 \, \text{mm yr}^{-1}$ and $V_G = 0.58 \pm 0.15 \, \text{mm yr}^{-1}$). The former estimate is within the observational uncertainty cited in the second IPCC report[1] ($V_O = 0.2$–$0.7 \, \text{mm yr}^{-1}$ and magnitude of $V_A < 1.4 \, \text{mm yr}^{-1}$), while the latter is higher (by just over 1–σ) than the upper bound cited for V_G ($0.4 \, \text{mm yr}^{-1}$).

Tide gauge records of sea-level change contain more information than has been recognized in previous studies of global sea-level rise. We have shown that geographic trends in (GIA-corrected) tide gauge rates at a set of carefully selected sites can be reconciled by invoking non-eustatic sea-level variations caused by continuing ice mass variations. We have furthermore demonstrated that it is possible to derive not only a single 'eustatic' measure of sea-level change but also, at least in principle, the independent contributions to this value from a subset of the various reservoirs of global ice. Our analysis is preliminary in several respects. First, ocean thermal expansion is clearly not a eustatic process[1], and our future work will incorporate a more realistic treatment of the process once its spatial geometry is better described[28]. If significant latitudinal gradients in the geometry of thermal expansion exist within the Northern Hemisphere then these will influence our estimate of the amplitude of Greenland mass flux. Second, we have focused on a restricted set of tide gauge sites, and in future work we will cautiously extend our procedure in order to incorporate a larger number of robust tide gauge records. □

1. Warrick, R. A., Le Provost, C., Meier, M. F., Oerlemans, J. & Woodworth, P. L. in *The Science of Climate Change: Contribution of Working Group I to the Second Assessment Report of the Intergovernmental Panel on Climate Change* (eds Houghton, J. T. *et al.*) 361–405 (Cambridge Univ. Press, Cambridge, 1990).
2. Woodworth, P. L., Pugh, D. T., De Ronde, J. G., Warrick, R. A. & Hannah, J. (eds) *Sea Level Changes: Determination and Effects* (American Geophysical Union, Washington, 1992).
3. Warrick, R. A., Barrow, E. M. & Wigley, T. M. L. (eds) *Climate and Sea Level Change: Observations, Projections and Implications* (Cambridge Univ. Press, Cambridge, 1993).
4. Peltier, W. R. & Tushingham, A. M. Global sea-level rise and the greenhouse effect: Might they be connected? *Science* 244, 806–810 (1989).
5. Douglas, B. C. Global sea level rise. *J. Geophys. Res.* 96, 6981–6992 (1991).
6. Peltier, W. R. & Tushingham, A. M. Influence of glacial isostatic adjustment on tide gauge measurements of secular sea level change. *J. Geophys. Res.* 96, 6779–6796 (1991).
7. Trupin, A. S. & Wahr, J. M. Spectroscopic analysis of global tide gauge sea level data. *Geophys. J. Int.* 100, 441–453 (1990).
8. Douglas, B. C. Global sea level rise: A redetermination. *Surv. Geophys.* 18, 279–292 (1997).
9. Peltier, W. R. Postglacial variations in the level of the sea: Implications for climate dynamics and solid-Earth geophysics. *Rev. Geophys.* 36, 603–689 (1998).
10. Woodward, R. S. On the form and position of mean sea level. *US Geol. Surv. Bull.* 48, 87–170 (1888).
11. Daly, R. A. Pleistocene changes of sea level. *Am. J. Sci.* 10, 281–313 (1925).
12. Farrell, W. E. & Clark, J. T. On postglacial sea level. *Geophys. J. R. Astron. Soc.* 46, 647–667 (1976).
13. Meier, M. F. Contribution of small glaciers to global sea level. *Science* 226, 1418–1421 (1984).
14. Milne, G. A., Mitrovica, J. X. & Davis, J. L. Near-field hydro-isostasy: The implementation of a revised sea-level equation. *Geophys. J. Int.* 139, 464–482 (1999).
15. Dziewonski, A. M. & Anderson, D. L. Preliminary reference Earth model (PREM). *Phys. Earth Planet. Inter.* 25, 297–356 (1981).
16. James, T. S. & Ivins, E. R. Global geodetic signatures of the Antarctic ice sheet. *J. Geophys. Res.* 102, 605–633 (1997).
17. Bentley, C. R. & Giovinetto, M. B. in *Proceedings of the International Conference on the Role of the Polar Regions in Global Change* (eds Weller, G., Wilson, C. L. & Severin, B. A. B.) 481–488 (Univ. Alaska, Fairbanks, 1991).
18. Jacobs, S. S., Hellmer, H. H., Doake, C. S. M., Jenkins, A. & Frolich, R. M. Melting of ice shelves and the mass balance of Antarctica. *J. Glacial.* 38, 375–387 (1992).
19. Krabill, W. *et al.* Greenland ice sheet: High-elevation balance and peripheral thinning. *Science* 289, 428–430 (2000).
20. Spencer, N. E. & Woodworth, P. L. *Data Holdings of the Permanent Service for Mean Sea Level* (Permanent Service for Mean Sea Level, Bidston, Birkenhead, 1993).
21. Plag, H.-P. & Jüttner, H.-U. Inversion of global tide gauges for present-day ice-load changes. *Proc. 2nd Int. Symp. Environ. Res. Arctic.* (in the press).
22. Tushingham, A. M. & Peltier, W. R. Ice-3G: A new global model of late Pleistocene deglaciation based upon geophysical predictions of postglacial relative sea level. *J. Geophys. Res.* 96, 4497–4523 (1991).
23. Davis, J. L. & Mitrovica, J. X. Glacial isostatic adjustment and the anomalous tide gauge record of eastern North America. *Nature* 379, 331–333 (1996).
24. Shennan, I. & Woodworth, P. L. A comparison of late Holocene and twentieth-century sea level trends from the UK and North Sea region. *Geophys. J. Int.* 109, 96–105 (1992).
25. Woodworth, P. L., Tsimplis, M. N., Flather, R. A. & Shennan, I. A review of the trends observed in British Isles mean sea level data measured by tide gauges. *Geophys. J. Int.* 136, 651–670 (1999).
26. Lambeck, K., Smither, C. & Ekman, M. Tests of glacial rebound models for Fennoscandinavia based on

instrumented sea- and lake-level records. *Geophys. J. Int.* 135, 375–387 (1998).
27. Trupin, A. S., Meier, M. F. & Wahr, J. M. Effect of melting glaciers on the Earth's rotation and gravitational field: 1965–1984. *Geophys. J. Int.* 108, 1–15 (1992).
28. Levitus, S., Antonov, J. L., Boyer, T. P. & Stephen, C. Warming of the global ocean. *Science* 287, 2225–2229 (2000).
29. Mitrovica, J. X. & Peltier, W. R. On postglacial geoid subsidence over the equatorial oceans. *J. Geophys. Res.* 96, 20053–20071 (1991).

....

Geological constraints on tidal dissipation and dynamical ellipticity of the Earth over the past three million years

Lucas J. Lourens*, Rolf Wehausen† & Hans J. Brumsack†

* *Faculty of Earth Sciences, Utrecht University, Budapestlaan 4, 3584 CD Utrecht, Netherlands*
† *Institute of Chemistry and Biology of the Marine Environment (ICBM), Carl von Ossietzky-University Oldenburg, PO Box 2503, D-26111 Oldenburg, Germany*

....

The evolution of the Solar System has been shown to be chaotic[1], which limits our ability to retrace the orbital and precessional motion of the Earth over more than 35–50 Myr (ref. 2). Moreover, the precession, obliquity and insolation parameters[3,4] can also be influenced by secular variations in the tidal dissipation and dynamical ellipticity of the Earth induced by glacial cyclicity[3,5–10] and mantle convection[11]. Here we determine the average values of these dissipative effects over the past three million years. We have computed the optimal fit between an exceptional palaeoclimate record from the eastern Mediterranean Sea and a model of the astronomical and insolation history[3] by testing a number of values for the tidal dissipation and dynamical ellipticity parameters. We find that the combined effects of dynamical ellipticity and tidal dissipation were, on average, significantly lower over the past three million years, compared to their present-day values (determined from artificial satellite data and lunar ranging[3,4,12]). This secular variation associated with the Plio-Pleistocene ice load history has caused an average acceleration in the Earth's rotation over the past 3 Myr, which needs to be considered in the construction of astronomical timescales and in research into the stationarity of phase relations in the ocean–climate system through time.

The main source of uncertainty in the computation of the precession and obliquity time series over the past three million years comes from changes in the Earth's dynamical ellipticity (E_D) due to surface mass load variations and tidal dissipation (TD) associated with the late Pliocene and Pleistocene ice-age cycles[3]. In particular, a change in E_D of about 0.00223 to that of the present-day could drive the precession and obliquity frequencies into resonance with a small perturbation term $s_6 - g_6 + g_5$ associated with Jupiter and Saturn[3]. Such a change in E_D can be reached during an ice age if the Earth would behave as a non-deformable (rigid) body[3]. But

1029